

図4. “Dual-targeting” リポソームの癌治療効果

Colon26 NL-17 大腸癌を移植したマウスを用いて “dual-targeting” リポソームの癌治療効果を検討した。無治療群として PBS 溶液 (●), 治療群としては PEG リポソーム (○), APPPG リポソーム (▲), NGR リポソーム (△), そして dual-targeting リポソーム (■) を投与した。投与スケジュールは, Colon26 NL-17 細胞を皮下移植 8 日後から各サンプルを中 2 日で 4 回, 1 回の投与につき DOX 投与量で 3 mg/kg とするよう尾静脈内投与した (矢印が投与日を表わしている)。“dual-targeting” リポソームは最も優れた癌治療効果を示した。

(* : p<0.05, *** : p<0.001). (文献 11 より引用)

されてきたが、アデノシンデアミナーゼ(ADA)欠損症などごく一部の疾患を除いて期待されたような効果は、なかなか得られていない。しかし、科学の進歩によって RNA 干渉(RNA interference ; RNAi)という革新的な遺伝子発現制御技術が誕生し、small interfering RNA (siRNA) や microRNA (miRNA) が核酸医薬の主役になる可能性が出てきている。過去には実用化が困難であろうと考えられていた抗体医薬品の市場が拡大を続けているように、核酸医薬においてもブレイクスルーとなるような技術革新、つまり siRNA の登場を機にして実用化が飛躍的に進む可能性がある。siRNA は、細胞内在性の遺伝子発現抑制システムを利用するために、従来のアンチセンス DNA 等の遺伝子制御技術と比較して非常に低濃度で選択的に遺伝子発現を抑制できる事が知られている。医薬品シーズとしての期待が大きく、企業における創薬研究も盛んである。しかし、siRNA は RNase によって体内で速やかに分解される事や細胞膜をほとんど透過しない事などから、siRNA を薬にするためには DDS 技術が不可欠となる。

siRNA を用いた RNA 干渉の特徴を極力活かせるベクターとして我々が注目しているのが非ウイルスベクターであり、リポソームがその 1 つである。研究用

試薬としては、すでに多くのカチオンリポソームが RNA 干渉実験用に市販されている。RNA 干渉を引き起こす方法としては、ウイルスやプラスミド DNA を用いた遺伝子導入により short hairpin RNA (shRNA) を発現させる方法もあるが、siRNA を “単純に載せる” 事ができるのは、非ウイルスベクターである。siRNA が一般的な医薬品と同様に、投与量や投与方法によってその効果や副作用を制御できるのに対し、shRNA の場合はそれらに加えて遺伝子発現の制御が必要になるであろう。また、shRNA が高分子の DNA を核内へデリバリーする必要があるのに対し、siRNA は比較的 low molecular weight であり、しかも細胞質にデリバリーすればよい。当然のことだが、siRNA の場合は遺伝子のどこに組み込まれるか心配する必要がない。更に、siRNA が容易に合成可能な低分子である事は製造技術的な大きなメリットであり、これは実用化に直結する重要な要素である。こうした数々の siRNA の良さを活かせるような非ウイルスベクターの開発が医療応用には欠かせない。すなわち siRNA 医薬品の開発においては、治療標的分子はもちろんのこと、siRNA デリバリーシステムの開発が成否の鍵となる。

In vitro で siRNA を細胞に導入する場合には、市販の研究用試薬で十分な事が多いが、治療目的となる



とクリアしなければならないハードルが飛躍的に高くなる。生体において標的組織に必要な量の siRNA を送達し、十分な治療効果を得るだけの遺伝子ノックダウンを実現するベクターには、高い導入効率、安定性、細胞選択性、安全性等が要求される。そこで我々は、siRNA の医療応用を念頭におき、導入ベクターとしてポリカチオンリポソーム (polycation liposomes ; PCL) の開発を進めてきた¹²⁾⁻¹⁴⁾。我々は、これまでに PCL がポリカチオンおよびカチオニックリポソームの両者の利点を併せ持つ、優れた siRNA 導入ベクターである事を明らかにしてきた¹⁴⁾。PCL は、カチオニックリポソームが持つ細胞内移行促進効果とポリカチオンが持つプロトンスポンジ効果(エンドソームから細胞質への核酸放出効果)によって優れたノックダウン効率を示す事が示唆されている。近年では PCL のポリカチオン部分について siRNA 導入に適した構造を探索し、新しい素材の開発を進めている。siRNA 導入ベクターに関する我々の研究成果の一部は既に論文化されているので、ご興味のある方は参照されたい^{14),15)}。ところで、PCL は一般のリポソームと同様、生体内安定性を向上するための PEG 修飾や標的細胞への特異性を付与するためのリガンド修飾等が容易である。従って、PCL は全身性投与(静脈内投与)を目的とした治療用ベクターとしても製剤設計が可能である。我々は、癌新生血管を標的とした siRNA ベクターとして、siRNA を搭載した PCL の表面を PEG と新生血管標的化ペプチドで修飾したベクターを開発し、動物実験において静脈内投与による siRNA デリバリーについて報告してきた。

現在、siRNA 医薬品の開発においては、眼の疾患である加齢性黄斑変性症など、局所投与が可能な疾患の方が臨床試験のステージが進んでいる。しかし、siRNA 医薬が抗体医薬のように市場を拡大し、広く医療に貢献するためには全身性投与で治療効果を得るところまで科学技術の進歩が必要であると考えられる。それを実現する可能性のある DDS 技術の 1 つとしてリポソームが挙げられる。

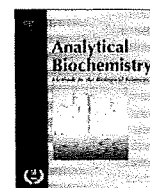
おわりに

本稿では、ここ 5~6 年の間に国内でも承認されるようになったリポソーム医薬品の話題や、次世代のリポソーム製剤の話題を中心に、その最新動向について紹介した。今回は取り上げなかったが、近年のリポソーム応用研究の動向としては、様々な疾患領域への展開が目覚ましい事が挙げられる。現在でも癌治療薬開発におけるリポソーム研究が多いのは変わらないが、国内では循環器領域や眼科領域などでの応用研究の進展が目立っている¹⁶⁾(循環器領域での DDS は『血管医学』Vol.10 No.3 p73-77 の南野先生の稿を参照)。また、メディカルエレクトロニクスとリポソームを組み合わせた研究も、臨床応用への期待が大きい(本誌の小玉先生の稿 p00 を参照)。その他としては、リポソーム技術を利用した人工赤血球や人工血小板のような人工血液成分に関する研究も、実用化が期待されている分野である。

本稿で述べてきたように、リポソーム技術は実際に医療に貢献する事のできる、いわゆるナノテクノロジーであるが、ほんの少し前までは国内でリポソームが薬になるのか、懐疑的な見方もあったように思う。動物実験で非常にいいデータを出してもなかなか医療への貢献に繋がらない、そのような歯がゆさを経験してきた DDS 研究者は少なくないはずである。現実問題として、科学的根拠とは関係ない知的財産権や薬価の問題も絡んで実用化が難しかった側面もあると思う。しかし、ようやく国内においてもリポソーム医薬品が医療に貢献するようになり、リポソームの医療応用の機運が高まりつつある。次世代医薬品として期待が大きい siRNA 医薬に DDS 技術が欠かせない事も後押ししているかもしれない。今後は、日本発のリポソーム医薬品の誕生に期待したいところであり、我々の研究がそれに少しでも寄与できれば幸甚であると考えている。

◎文 献

- 1) リポソーム応用の新展開～人工細胞の開発に向けて～(秋吉一成, 辻井 薫 監修). 株式会社エヌ・ティー・エス, 東京, 2005
- 2) Matsumura Y, Maeda H : A new concept for macromolecular therapeutics in cancer chemotherapy : Mechanism of tumorotropic accumulation of proteins and the antitumor agent SMANCS. *Cancer Res* **46** : 6387-6392, 1986
- 3) Maeda N, Miyazawa S, Shimizu K, et al : Enhancement of anticancer activity in antineovascular therapy is based on the intratumoral distribution of the active targeting carrier for anticancer drugs. *Biol Pharm Bull* **29** : 1936-1940, 2006
- 4) Oku N, Asai T, Watanabe K, et al : Anti-neovascular therapy using novel peptides homing to angiogenic vessels. *Oncogene* **21** : 2662-2669, 2002
- 5) Maeda N, Takeuchi Y, Takada M, et al : Anti-neovascular therapy by use of tumor neovasculature-targeted long-circulating liposome. *J Control Release* **100** : 41-52, 2004
- 6) Yonezawa S, Asai T, Oku N : Effective tumor regression by anti-neovascular therapy in hypovascular orthotopic pancreatic tumor model. *J Control Release* **118** : 303-309, 2007
- 7) Shimizu K, Asai T, Oku N : Antineovascular therapy, a novel antiangiogenic therapy. *Expert Opin Ther Targets* **9** : 63-76, 2005
- 8) 浅井知浩 : 腫瘍新生血管標的化リポソームの新展開. *薬剤学* **65** : 169-174, 2005
- 9) 浅井知浩, 奥 直人 : リポソーム応用の新展開. *最新医学* **61** : 1084-1091, 2006
- 10) 浅井知浩, 米澤 正, 奥 直人 : 腫瘍新生血管標的化リポソーム. *Mebio Oncology* **4** : 48-57, 2007
- 11) Murase Y, Asai T, Katanasaka Y, et al : A novel DDS strategy. "dual-targeting", and its application for antineovascular therapy. *Cancer Lett* : 2009 (Epub ahead of print)
- 12) Pastorino F, Brignole C, Marimpietri D, et al : Vascular damage and anti-angiogenic effects of tumor vessel-targeted liposomal chemotherapy. *Cancer Res* **63** : 7400-7409, 2003
- 13) Sugiyama M, Matsuura M, Takeuchi Y, et al : Possible mechanism of polycation liposome (PCL)-mediated gene transfer. *Biochim Biophys Acta* **1660** : 24-30, 2004
- 14) Asai T, Suzuki Y, Matsushita S, et al : Disappearance of the angiogenic potential of endothelial cells caused by Argonaute2 knockdown. *Biochem Biophys Res Commun* **368** : 243-248, 2008
- 15) Hatanaka K, Shimizu K, Asai T, Oku N : Antineovascular gene therapy by Ago2 knockdown. *Yakugaku Zasshi* **128** : 1567-1575, 2008
- 16) Takahama H, Minamino T, Asanuma H, et al : Prolonged targeting of ischemic/reperfused myocardium by liposomal adenosine augments cardioprotection in rats. *J Am Coll Cardiol* **53** : 709-717, 2009



Bionanocapsule-based enzyme–antibody conjugates for enzyme-linked immunosorbent assay

Masumi Iijima^{a,b}, Takashi Matsuzaki^a, Hiroyasu Kadoya^a, Satoko Hatahira^c, Shingo Hiramatsu^c, Gimán Jung^c, Katsuyuki Tanizawa^{a,*}, Shun'ichi Kuroda^{a,b,*}

^a Institute of Scientific and Industrial Research, Osaka University, Ibaraki, Osaka 567-0047, Japan

^b Graduate School of Bioagricultural Sciences, Nagoya University, Chikusa, Nagoya 464-8601, Japan

^c New Frontiers Research Laboratories, Toray Industries, Kamakura, Kanagawa 248-8555, Japan

ARTICLE INFO

Article history:

Received 7 July 2009

Available online 9 October 2009

Keywords:

ELISA

IgG

Protein A

Nanoparticles

Oriented immobilization

ABSTRACT

Macromolecules that can assemble a large number of enzyme and antibody molecules have been used frequently for improvement of sensitivities in enzyme-linked immunosorbent assays (ELISAs). We generated bionanocapsules (BNCs) of approximately 30 nm displaying immunoglobulin G (IgG) Fc-binding ZZ domains derived from *Staphylococcus aureus* protein A (designated as ZZ-BNC). In the conventional ELISA using primary antibody and horseradish peroxidase-labeled secondary antibody for detecting antigen on the solid phase, ZZ-BNCs in the aqueous phase gave an approximately 10-fold higher signal. In Western blot analysis, the mixture of ZZ-BNCs with secondary antibody gave an approximately 50-fold higher signal than that without ZZ-BNCs. These results suggest that a large number of secondary antibody molecules are immobilized on the surface of ZZ-BNCs and attached to antigen, leading to the significant enhancement of sensitivity. In combination with the avidin–biotin complex system, biotinylated ZZ-BNCs showed more significant signal enhancement in ELISA and Western blot analysis. Thus, ZZ-BNC is expected to increase the performance of various conventional immunoassays.

© 2009 Elsevier Inc. All rights reserved.

Enzyme immunoassay (EIA),¹ radioimmunoassay (RIA), and fluoroimmunoassay (FIA) have been widely used for high-throughput screening of immunocomplexes. To increase the sensitivity of these immunoassays, two types of macromolecules have been used in the reaction with antibody. One type of macromolecule allows clustering of antibodies and labeling molecules (e.g., enzyme, radioactive material, fluorescence). For example, polymeric horseradish peroxidase (HRP)–streptavidin conjugate [1], 3DNA dendrimer [2], and immunoglobulin G (IgG)–poly-D-glutamic acid–(HRP)_n conjugate [3] have been used previously. However, these macromolecules require chemical modification of antibodies and do not allow the oriented immobilization of antibodies [4] that improves the avidity and anti-

gen recognition of antibodies [5]. In general, chemical modification is considered to reduce the stability or antigen-binding activity of antibodies. Another type of macromolecule is expected to permit the oriented immobilization of antibodies. For example, nanoparticles have been used for displaying antibodies on their surface (e.g., streptavidin-conjugated nanobeads [6], biotin-coated liposomes [7]). Because biotinylation occurred randomly at free amino groups on the surface of antibodies, these nanoparticles partially accomplished oriented immobilization of antibodies using an avidin–biotin complex (ABC). These results encouraged us to develop macromolecules that can assemble antibodies and labeling molecules without chemical modification in the manner of oriented immobilization.

On the other hand, we previously developed a yeast-derived hollow nanoparticle applicable for pinpoint delivery of drugs and genes [8]. The nanoparticle, bionanocapsule (BNC), has a diameter of approximately 30 nm and is composed of hepatitis B virus (HBV) surface antigen (HBsAg) L proteins embedded in a liposome [9]. The L protein is a three-membrane-spanning protein possessing a pre-S region at the N terminal of the S region (see Fig. 1A) [10]. BNCs can incorporate various therapeutic materials (e.g., drugs, genes) by electroporation [8] and liposome fusion [11] and can deliver them specifically to the human liver [8] based on the liver-specific recognition ability of the pre-S region [12]. Recently, to alter the tissue specificity of BNC, our collaborators made a

* Corresponding authors. Fax: +81 6 6879 8460 (K. Tanizawa), +81 52 789 5227 (S. Kuroda).

E-mail addresses: tanizawa@sanken.osaka-u.ac.jp (K. Tanizawa), skuroda@agr.nagoya-u.ac.jp (S. Kuroda).

¹ Abbreviations used: EIA, enzyme immunoassay; RIA, radioimmunoassay; FIA, fluoroimmunoassay; HRP, horseradish peroxidase; IgG, immunoglobulin G; ABC, avidin–biotin complex; BNC, bionanocapsule; HBV, hepatitis B virus; HBsAg, HBV surface antigen; ZZ-BNC, IgG Fc-interacting region (Z domain) derived from *Staphylococcus aureus* protein A; ELISA, enzyme-linked immunosorbent assay; TEM, transmission electron microscopy; OVA, ovalbumin; PBS, phosphate-buffered saline; TMB, 3,3',5,5'-tetramethylbenzidine; IgE, immunoglobulin E; PVDF, polyvinylidene fluoride; EGFR, epidermal growth factor receptor; EGFP, enhanced green fluorescent protein; LOD, limit of detection; SD, standard deviations; LOQ, limit of quantitation.

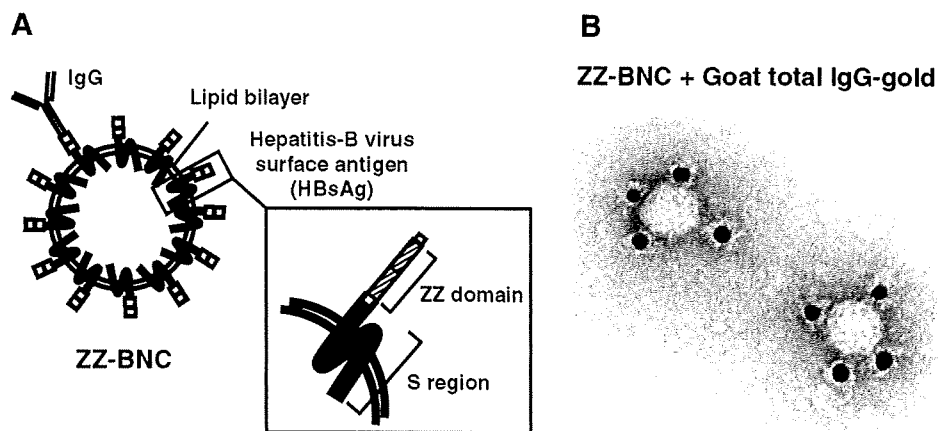


Fig. 1. (A) Schematic structure of a ZZ-BNC. (B) Transmission electron microscopy (TEM) images of ZZ-BNC conjugated with 10-nm gold particle-labeled goat total IgG. Bar = 40 nm.

derivative of BNC by replacing the pre-S region with a tandem sequence of the IgG Fc-interacting region (Z domain) derived from *Staphylococcus aureus* protein A [13] and designated it ZZ-BNC [14] (Fig. 1A). ZZ-BNC allowed us to display antibodies on its surface and to deliver various therapeutic materials to tissues of interest in an antibody-dependent manner [14].

These properties led us to imagine that ZZ-BNC spontaneously adsorbs antibodies in the manner of oriented immobilization. In this study, we examined whether ZZ-BNCs could contribute to signal enhancement of enzyme-linked immunosorbent assay (ELISA) through formation of IgG-ZZ-BNC complexes.

Materials and methods

ZZ-BNCs

ZZ-BNCs were overexpressed in *Saccharomyces cerevisiae* AH22R⁻ carrying the ZZ-BNC expression plasmid pGLD-ZZ50 [14]. According to the preparation method for BNCs [8], ZZ-BNCs were extracted by the disruption with glass beads and purified using an AKTA chromatography system (GE Healthcare, Amersham, UK) by affinity chromatography on porcine IgG and gel filtration.

Transmission electron microscopy

ZZ-BNCs (1 μ g as protein) were mixed with 10-nm gold particle-labeled goat total IgG (50 μ l, Sigma-Aldrich, St. Louis, MO, USA), adsorbed onto a carbon-coated copper grid (JEOL, Tokyo, Japan), negatively stained using 2% (w/v) phosphotungstic acid (pH 7.0), and subjected to transmission electron microscopy (TEM) using a model JEM1011 (Jeol).

ELISA for ovalbumin on solid phase

Ovalbumin (OVA, 100 μ l, 0–6.25 ng/ml, Sigma-Aldrich) was adsorbed to each well of a Nunc-Immuno Plate II (96 wells, Nalge Nunc International, Rochester, NY, USA). The plate was kept at 4 °C overnight and washed three times with PBST (200 μ l of phosphate-buffered saline [PBS], 137 mM NaCl, 2.7 mM KCl, 10 mM Na₂PO₄, and 2 mM KH₂PO₄ [pH 7.4] containing 0.05% [v/v] Tween 20). Antibodies were diluted with PBST containing 5% (w/v) skimmed milk (Nacalai Tesque, Kyoto, Japan). A primary antibody, a mouse anti-OVA IgG₁ antibody (100 μ l, 0.4 μ g/ml, Abcam, Cambridge, UK), was added to each well, incubated at room tempera-

ture for 1.5 h, and washed three times with PBST. A secondary antibody, HRP-conjugated rabbit anti-mouse IgG (100 μ l, 2 μ g/ml, Sigma-Aldrich), was added to each well, incubated at room temperature for 1.5 h, and washed three times with PBST. When biotinylated rabbit anti-mouse IgG (100 μ l, 2 μ g/ml, Sigma-Aldrich) was used as the secondary antibody, the ABC system (ABC peroxidase staining kit, Pierce, Rockford, IL, USA) was used for the labeling with HRP. The colorimetric reaction was carried out at room temperature for 15 min in 100 μ l per well of a 3,3',5,5'-tetramethylbenzidine (TMB) substrate kit (Pierce). The reaction was stopped with 100 μ l of 2 N H₂SO₄. Absorbance at 450 nm was measured on a Varioskan microplate reader (Thermo Fisher Scientific, Waltham, MA, USA) using absorbance at 690 nm as the reference. When the calibration curve was generated using 0–6.25 ng/ml OVA ($n = 8$), the wells containing 0 ng/ml OVA were defined as blank wells for subtracting background.

ELISA for anti-OVA immunoglobulin E antibodies in aqueous phase

OVA (100 μ l, 15 μ g/ml) was adsorbed onto each well of a Nunc-Immuno Plate II. The plate was kept at 4 °C overnight and washed three times with 200 μ l of PBST. Mouse anti-OVA immunoglobulin E (IgE) antibody (0–6.25 ng/ml, 100 μ l, AbD Serotec, Oxford, UK) diluted with PBST containing 5% skimmed milk was added to each well, incubated at room temperature for 1.5 h, and washed three times with PBST. An HRP-conjugated rabbit anti-mouse IgE Fc antibody (100 μ l, 5 μ g/ml, Nordic Immunological Laboratories, Tilburg, Netherlands) was added to each well, incubated at room temperature for 1.5 h, and washed three times with PBST. When biotin-labeled rabbit anti-mouse IgE Fc antibody (100 μ l, 5 μ g/ml, Nordic Immunological Laboratories) was used as the secondary antibody, the ABC peroxidase staining kit was used for the labeling with HRP. The colorimetric reaction was carried out at room temperature for 15 min in 100 μ l per well of a TMB substrate kit. The reaction was stopped with 100 μ l of 2 N H₂SO₄. Absorbance at 450 nm was measured on a Varioskan microplate reader using absorbance at 690 nm as the reference. When the calibration curve was generated using 0–6.25 ng/ml anti-OVA IgE ($n = 8$), the wells containing 0 ng/ml anti-OVA IgE were defined as blank wells for subtracting background.

Western blot analysis

Here 1 μ l of OVA (0.001–10 mg/ml) was blotted onto a polyvinylidene fluoride (PVDF) membrane (Millipore, Billerica, MA,

USA) and dried at room temperature for 30 min. The membrane was blocked with 5% skimmed milk in TBST (20 mM Tris-HCl, 140 mM NaCl, and 0.05% Tween 20 [pH 7.4]) at room temperature for 30 min and then incubated at room temperature for 1 h with the mouse anti-OVA IgG₁ antibody (1 µg/ml) diluted with TBST. The membrane was washed three times with TBST and incubated with the HRP-conjugated rabbit anti-mouse IgG (1 µg/ml) at room temperature for 1 h. When biotinylated rabbit anti-mouse IgG (1 µg/ml) was used as the secondary antibody, the ABC system was used for the labeling with HRP. After washing three times with TBST, the membrane was treated with ECL Western blotting detection reagents (GE Healthcare) and then the immunoreactive spots were visualized under a luminescence image analyzer (LAS-4000mini, Fujifilm, Tokyo, Japan).

Results and discussion

Display of antibodies on ZZ-BNC surface

BNC is a yeast-derived hollow nanocapsule consisting of approximately 110 HBsAg L proteins embedded in a liposome [8]. Recently, we replaced the N-terminal region of L protein (pre-S region) with a tandem sequence of protein A-derived IgG Fc-binding domain (Z domain) and designated it ZZ-BNC [14] (Fig. 1A). When mixed with anti-EGFR (epidermal growth factor receptor) antibody, the ZZ-BNCs labeled with enhanced green fluorescent protein (EGFP) accumulated on the surface of human cervical carcinoma HeLa cells that express EGFR abundantly [14]. Therefore, we mixed ZZ-BNC with 10-nm gold particle-labeled goat total IgG and observed it under TEM. As shown in Fig. 1B, approximately 30-nm ZZ-BNCs were surrounded by several molecules of 10-nm gold particle-labeled goat total IgG. This result strongly suggested that Z domains surrounding the ZZ-BNC surface tether the

IgG Fc domains to display all IgG Fv regions outward for effective antigen binding. Thus, ZZ-BNC was expected to cluster antibodies on its surface in the manner of oriented immobilization, which might improve the avidity and antigen recognition of antibodies [5].

ELISA for antigens on solid phase

The enhancement of the sensitivity was examined in the detection of antigen (OVA) by ELISA with or without ZZ-BNCs (see Fig. 2A, panels 1 and 2). As described in Materials and methods, OVA (0–6.25 ng/ml) was adsorbed onto each well of the immunoplate, contacted with primary antibody, and then contacted with secondary antibody (see Fig. 2A, panel 1). When the purified ZZ-BNCs (2 µg/ml as protein) were preincubated with the secondary antibody (2 µg/ml) at room temperature for 30 min and then added to each well (see Fig. 2A, panel 2), the signal at 3.125 ng/ml OVA was approximately 10-fold higher than that without ZZ-BNCs (Fig. 2B, lines 1 and 2). The ABC system has been widely used for the enhancement of ELISA signals because it forms a tetrameric avidin-based complex of biotinylated antibodies and biotinylated HRP (see Fig. 2A, panel 3). The signal at 3.125 ng/ml OVA with the ABC system was approximately 4-fold higher than that with the conventional ELISA (Fig. 2B, lines 1 and 3). When ZZ-BNC (2 µg/ml as protein) was preincubated with the biotinylated secondary antibody (2 µg/ml) at room temperature for 30 min and then added to each well (100 µl) (see Fig. 2A, panel 4), the signal at 3.125 ng/ml OVA was approximately 13-fold higher than that without ZZ-BNCs or the ABC system (Fig. 2B, lines 1 and 4). Next, biotinylated ZZ-BNCs (2 µg/ml as protein) were prepared with EZ-Link Sulfo-NHS-Biotin (Pierce) according to the manufacturer's protocol and added to the secondary antibody instead of ZZ-BNCs (see Fig. 2A, panel 5). The signal at 3.125 ng/ml OVA was approximately 19-fold higher than that without ZZ-BNCs or the ABC sys-

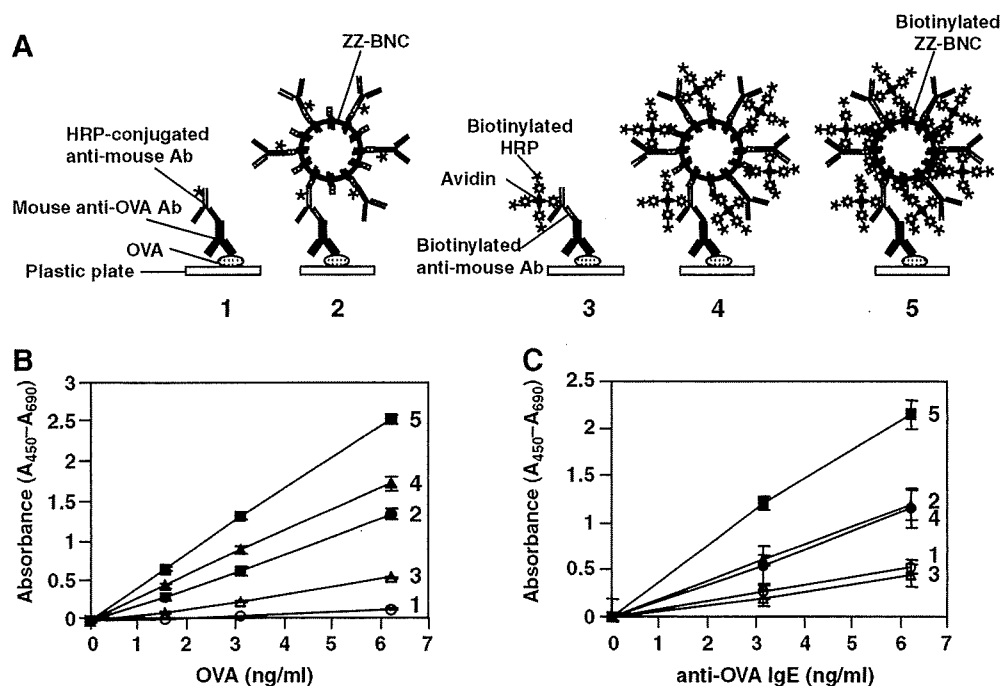


Fig. 2. (A) Schematic representations of various ELISA systems for OVA detection. Panel 1: conventional ELISA using an anti-OVA antibody and an HRP-conjugated anti-mouse IgG antibody; panel 2: conventional ELISA in the presence of ZZ-BNC; panel 3: conventional ELISA with the ABC system; panel 4: conventional ELISA with the ABC system in the presence of ZZ-BNCs; panel 5: conventional ELISA with the ABC system in the presence of biotinylated ZZ-BNC. Ab, antibody. (B) Detection of OVA (solid phase) by various ELISA systems. Results are means \pm SD ($n = 8$). Numbers correspond to the methods shown in panel (A). (C) Detection of anti-OVA IgE (aqueous phase) by various ELISA systems. Results are means \pm SD ($n = 8$). Numbers correspond to the methods shown in panel (A).

tem (Fig. 2B, lines 1 and 5). The sensitivity for ELISA is defined by the limit of detection (LOD, mean \pm 3SD [standard deviations]) and the limit of quantitation (LOQ, mean \pm 10SD) [15] at the lowest end of the quantifiable concentration range of OVA ($n = 20$). As shown in Table 1, the LOD and LOQ of ELISA (see Fig. 2A, panel 1, 750 and 1500 pg/ml, respectively) were decreased by 47% using ZZ-BNCs (see Fig. 2A, panel 2, 350 and 700 pg/ml, respectively), indicating that the two sensitivities (LOD and LOQ) were increased 2.1-fold. The ABC system enhanced the two sensitivities 2.5- and 20-fold in the presence of ZZ-BNCs (see Fig. 2A, panel 4) and biotinylated ZZ-BNCs (see Fig. 2A, panel 5), respectively.

ELISA for antibodies in aqueous phase

We investigated the enhancement of the sensitivity of detection of the primary antibody by ELISA using ZZ-BNCs and biotinylated ZZ-BNCs. OVA adsorbed onto each well was contacted with primary antibody (0-6.25 ng/ml) and then contacted with secondary antibody (see Materials and methods and Fig. 2A, panel 1). When ZZ-BNC (1.25 μ g/ml as protein) was preincubated with the secondary antibody (5 μ g/ml) at room temperature for 30 min and then added to each well (see Fig. 2A, panel 2), the signal at 3.125 ng/ml mouse anti-OVA IgE antibody was 2.3-fold higher than that without ZZ-BNCs (Fig. 2C, lines 1 and 2). Next, with the concurrent use of biotinylated secondary antibody (5 μ g/ml), biotinylated ZZ-BNCs (2.5 μ g/ml as protein), and the ABC system, the signal at 3.125 ng/ml mouse anti-OVA IgE antibody was 4.4-fold higher than that of conventional ELISA (Fig. 2C, lines 1 and 5). Furthermore, the sensitivity for ELISA is defined by the LOD and LOQ [15] at the lowest end of the quantifiable concentration range of anti-OVA IgE ($n = 20$). The LOD was decreased by 50% and 8% using ZZ-BNCs and biotinylated ZZ-BNCs, respectively (Table 1).

Western blot analysis

Signal enhancement of ELISA for antigens on solid phase by ZZ-BNCs led us to examine whether they are applicable for Western blot analysis. The dot blot containing OVA (from 1 ng/spot to 10 μ g/spot) was incubated with the primary antibody at room temperature for 1 h, incubated with the secondary antibody at room temperature for 1 h, and then subjected to chemiluminescence detection (see Materials and methods). When ZZ-BNCs (1 μ g/ml as protein) were preincubated with the secondary antibody (1 μ g/ml) at room temperature for 30 min, the spot containing 10 ng of OVA could be detected, which was approximately 50-fold higher than that without ZZ-BNCs (Fig. 3, lanes 1 and 2). Next, the use of the ABC system and biotinylated secondary antibody facilitated us to detect the spot containing 50 ng of OVA (Fig. 3, lane 3). The adaptation of ZZ-BNCs (1 μ g/ml as protein)

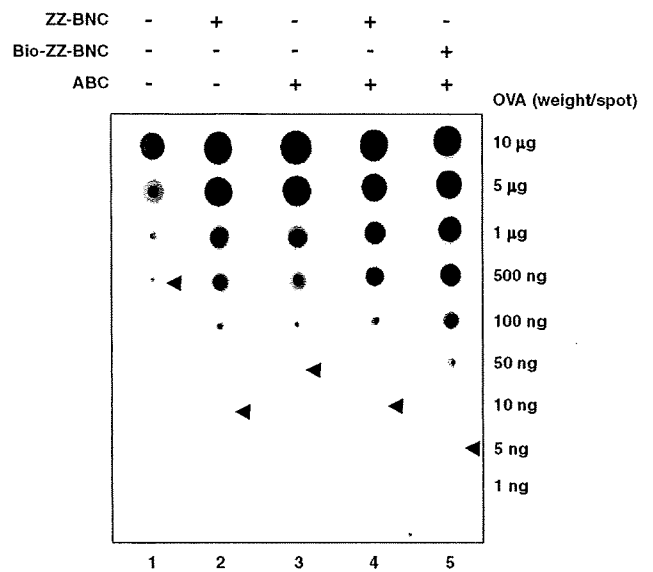


Fig. 3. Western blot analyses of spotted OVA by various detection methods. Lane numbers correspond to the methods shown in Fig. 2A. The minimum OVA amounts detectable by each method are indicated with arrowheads.

and biotinylated ZZ-BNCs (1 μ g/ml as protein) to this system achieved approximately 5- and 10-fold higher sensitivity (Fig. 3, lanes 4 and 5, respectively), comparable to 50- and 100-fold enhancements from the conventional method (lane 1). It was confirmed that the combined use of the ABC system and biotinylated ZZ-BNCs significantly enhanced the sensitivity of not only ELISA but also Western blot analysis. Furthermore, ZZ-BNCs might be applicable for the signal enhancement of immunohistochemical analysis.

Conclusions

It has been demonstrated that ZZ-BNCs could assemble antibodies on their surface even without chemical modification. ZZ-BNCs could then enhance the signals in the detection of antigens and antibodies when added to the aqueous phase of conventional ELISA and Western blot analysis. A combination of the ABC system and biotinylated ZZ-BNCs significantly improved the sensitivity of conventional ELISA and Western blot analysis. In Fig. 1B, ZZ-BNCs are shown to tether the Fc regions of IgG on the ZZ domain so that all of the Fv regions are displayed outward for effective formation of immunocomplexes. Thus, oriented immobilization of antibodies has presumably been achieved on the surface of ZZ-BNCs. As mentioned above, BNCs (including ZZ-BNCs) can incorporate various materials by electroporation and liposome fusion. This indicated that ZZ-BNCs may be applicable for RIA and FIA. BNCs could be adsorbed onto a mica surface without the disruption of its particle structure [16]. Therefore, ZZ-BNCs would also be applicable for the oriented immobilization of antibodies in the solid phase of various immunoassay systems.

Acknowledgments

We thank Profs. A. Kondo (Kobe University), M. Seno (Okayama University), and M. Ueda (Keio University) for helpful advice. This work was supported by the Research and Development Program for New Bio-industry Initiatives from the Bio-oriented Technology Research Advancement Institution (BRAIN) of Japan; the Research on Advanced Medical Technology from the Ministry of Health,

Table 1 Sensitivities of various ELISA systems for OVA.

Method	LOD (pg/ml) (mean \pm 3SD)	CV (%)	LOQ (pg/ml) (mean \pm 10SD)	CV (%)
<i>For detection of antigen (OVA)</i>				
Conventional ELISA	750	4.5	1500	3.4
+ ZZ-BNC	350	6.4	700	6.9
+ ABC	500	3.0	1000	3.1
+ ABC + ZZ-BNC	300	5.3	600	11.8
+ ABC + bio-ZZ-BNC	40	3.5	80	4.3
<i>For detection of primary antibody (anti-OVA IgE)</i>				
Conventional ELISA	500	5.0	ND	ND
+ ZZ-BNC	250	5.4	500	4.6
+ ABC + bio-ZZ-BNC	40	4.2	130	3.6

Note. bio-, biotinylated; ND, not detected.

Labor, and Welfare of Japan; and the Regional Research and Development Resources Utilization Program of the Japan Science and Technology Agency (JST).

References

- [1] R.G. Vasilov, E.N. Tsitsikov, An ultrasensitive immunoassay for human IgE measurement in cell-culture supernatant, *Immunol. Lett.* 26 (1990) 283–284.
- [2] J.R. Mora, T.L. Zielinski, B.P. Nelson, R.C. Getts, Protein detection enhanced by 3DNA dendrimer signal amplification, *BioTechniques* 44 (2008) 815–818.
- [3] B. Simons, H. Kaplan, M.A. Hefford, Novel cross-linked enzyme-antibody conjugates for Western blot and ELISA, *J. Immunol. Methods* 315 (2006) 88–98.
- [4] S.V. Rao, K.W. Anderson, L.G. Bachas, Oriented immobilization of proteins, *Mikrochim. Acta* 128 (1998) 127–143.
- [5] N.S. Lipman, L.R. Jackson, L.J. Trudel, F. Weis-Garcia, Monoclonal versus polyclonal antibodies: distinguishing characteristics, applications, and information resources, *ILAR J.* 46 (2005) 258–268.
- [6] Y. Teramura, Y. Arima, H. Iwata, Surface plasmon resonance-based highly sensitive immunosensing for brain natriuretic peptide using nanobeads for signal amplification, *Anal. Biochem.* 357 (2006) 208–215.
- [7] T. Wink, S.J. van Zuilen, A. Bult, W.P. van Bennekom, Liposome-mediated enhancement of the sensitivity in immunoassays of proteins and peptides in surface plasmon resonance spectrometry, *Anal. Chem.* 70 (1998) 827–832.
- [8] T. Yamada, Y. Iwasaki, H. Tada, H. Iwabuki, M.K. Chuah, T. VandenDriessche, H. Fukuda, A. Kondo, M. Ueda, M. Seno, K. Tanizawa, S. Kuroda, Nanoparticles for the delivery of genes and drugs to human hepatocytes, *Nat. Biotechnol.* 21 (2003) 885–890.
- [9] S. Kuroda, S. Otaka, T. Miyazaki, M. Nakao, Y. Fujisawa, Hepatitis B virus envelope L protein particles, *J. Biol. Chem.* 267 (1992) 1953–1961.
- [10] T. Nagaoka, T. Fukuda, S. Yoshida, H. Nishimura, D. Yu, S. Kuroda, K. Tanizawa, A. Kondo, M. Ueda, H. Yamada, H. Tada, M. Seno, Characterization of bionanocapsule as a transfer vector targeting human hepatocyte carcinoma by disulfide linkage modification, *J. Control. Release* 118 (2007) 348–356.
- [11] J. Jung, T. Matsuzaki, K. Tatematsu, T. Okajima, K. Tanizawa, S. Kuroda, Bionanocapsule conjugated with liposomes for in vivo pinpoint delivery of various materials, *J. Control. Release* 126 (2008) 255–264.
- [12] A.R. Neurath, S.B. Kent, N. Strick, K. Parker, Identification and chemical synthesis of a host cell receptor binding site on hepatitis B virus, *Cell* 46 (1986) 429–436.
- [13] B. Nilsson, T. Moks, B. Jansson, L. Abrahmsén, A. Elmlblad, E. Holmgren, C. Henrichson, T.A. Jones, M. Uhlén, A synthetic IgG-binding domain based on staphylococcal protein A, *Protein Eng.* 1 (1987) 107–113.
- [14] N. Kurata, T. Shishido, M. Muraoka, T. Tanaka, C. Ogino, H. Fukuda, A. Kondo, Specific protein delivery to target cells by antibody-displaying bionanocapsules, *J. Biochem.* 144 (2008) 701–707.
- [15] D. MacDougall, W.B. Crummett, Guidelines for data acquisition and data quality evaluation in environmental chemistry, *Anal. Chem.* 52 (1980) 2242–2249.
- [16] T. Kanno, T. Yamada, H. Iwabuki, H. Tanaka, S. Kuroda, K. Tanizawa, T. Kawai, Size distribution measurement of vesicles by atomic force microscopy, *Anal. Biochem.* 309 (2002) 196–199.



ELSEVIER

Available online at www.sciencedirect.com



nanomedicine

Nanomedicine: Nanotechnology, Biology, and Medicine xx (2010) xxx – xxx

www.nanomedjournal.com

Research Article: Medicine

Hepatoma-targeted gene delivery using a tumor cell-specific gene regulation system combined with a human liver cell-specific bionanocapsule

Jeong-Hun Kang, PhD^{a,1}, Jun Oishi, PhD^{a,b,1}, Jong-Hwan Kim, PhD^c, Moeko Ijuin, MD^{a,b}, Riki Toita, MD^{a,b}, Byungdug Jun, PhD^c, Daisuke Asai, PhD^d, Takeshi Mori, PhD^{a,b}, Takuro Niidome, PhD^{a,b,e}, Katsuyuki Tanizawa, PhD^f, Shun'ichi Kuroda, PhD^f, Yoshiki Katayama, PhD^{a,b,e,*}

^aDepartment of Applied Chemistry, Faculty of Engineering, Kyushu University, Fukuoka, Japan

^bGraduate School of Systems Life Sciences, Kyushu University, Fukuoka, Japan

^cFaculty of Education, Nagasaki University, Nagasaki, Japan

^dDepartment of Microbiology, St. Marianna University School of Medicine, Kawasaki, Japan

^eCenter for Future Chemistry, Kyushu University, Fukuoka, Japan

^fInstitute of Scientific and Industrial Research, Osaka University, Osaka, Japan

Received 4 July 2009; accepted 15 January 2010

Abstract

Hepatoma (hepatocellular carcinoma) is the most common type of malignant tumor originating in the liver and has a relatively low 5-year survival rate. The development of hepatoma-targeted therapy is needed to increase treatment efficiency and to reduce the incidence of undesirable side effects. In this study we developed a novel hepatoma-targeted gene delivery system. The gene delivery system was prepared by combining a human liver cell-specific bionanocapsule (BNC) and a tumor cell-specific gene regulation polymer, which responds to hyperactivated protein kinase C α in hepatoma cells. The complex of the polymer-DNA with BNCs was delivered into cells and tissues. The developed system showed increased transfection efficiency and resulted in cell-specific gene expression in hepatoma cells and tissues (HuH-7), but no gene expression in normal human hepatocytes or human epidermoid tumor cells (A431). The combination of a tumor cell-specific gene regulation system responding to protein kinase C α and BNCs showed excellent potential for the selective treatment of hepatomas. The system could be a useful method with applications in hepatoma-specific gene therapy and molecular imaging.

© 2010 Elsevier Inc. All rights reserved.

Key words: Protein kinase; Intracellular signal; Hepatocellular carcinoma; Gene delivery

Hepatoma (hepatocellular carcinoma) is the most common type of malignant tumor originating in the liver and has a relatively low 5-year survival rate (<10%).^{1,2} It is highly resistant to conventional chemotherapy and radiation therapy. Moreover,

because many conventional antitumor drugs are nonselective for hepatoma cells, they can cause undesirable side effects.^{3,4}

There has been a recent increase in interest in gene therapy as a new approach to hepatoma treatment. Viral and nonviral vectors are used to deliver therapeutic genes, mainly tumor suppressor (e.g., p53) and suicide genes (e.g., herpes simplex virus thymidine kinase), into hepatoma cells. However, problems arise, because the delivered gene is expressed both in targeted hepatoma cells and in nontargeted normal cells. Many targeting strategies using hepatoma-specific molecular markers, mainly membrane receptors, have been investigated with the aim of overcoming this problem.⁵⁻⁸

Our group has investigated the possible application of intracellular signal transduction pathways for disease-targeted

This work was supported in part by a Grant-in-Aid for Scientific Research from the Ministry of Education, Science, Sports and Culture of Japan.

*Corresponding author: Department of Applied Chemistry, Faculty of Engineering, Kyushu University, 744 Motooka, Nishi-Ku, Fukuoka 819-0395, Japan.

E-mail address: ykatatcm@mbox.nc.kyushu-u.ac.jp (Y. Katayama).

¹ These authors contributed equally to this work.

1549-9634/\$ – see front matter © 2010 Elsevier Inc. All rights reserved.
doi:10.1016/j.nano.2010.01.007

Please cite this article as: J.-H. Kang, et al, Hepatoma-targeted gene delivery using a tumor cell-specific gene regulation system combined with a human liver cell-specific bionanocapsule. *Nanomedicine: NBM* 2010;xx:1-7, doi:10.1016/j.nano.2010.01.007

gene therapy.^{9–11} Living cells make use of numerous intracellular signal transduction pathways that respond to extracellular signals and regulate or modulate gene expression. Phosphorylation by protein kinases has an important role in cellular growth and functions through activation of their target proteins in these intracellular signal transduction pathways. Abnormal activation of certain protein kinases has been reported in many diseases.^{12,13} If such hyperactivated protein kinases can be used to activate transgene expression, disease cell-specific gene regulation becomes possible.

Among the protein kinases, protein kinase C (PKC) is a phospholipid-dependent serine/threonine kinase that seems to be involved in the signal transduction response to a variety of hormones and growth factors. PKC isozymes are classified into three subfamilies based on structural and activation characteristics: conventional or classic PKCs (cPKCs; α , β I, β II, and γ), novel or nonclassic PKCs (nPKCs; δ , ϵ , η , and θ), and atypical PKCs (ζ , ι and λ). Among PKC isozymes, PKC α is over-expressed or hyperactivated in several cancer cells or tissues (e.g., hepatoma, breast cancer, and melanoma) but has negligible activity in other normal tissues.^{14–16}

We recently found a PKC α -specific substrate peptide that exhibited a higher phosphorylation ratio in tumor cells and tissues, compared with normal tissues.¹⁷ Moreover, we have developed a novel tumor-targeted gene regulation system responding to PKC α by using the PKC α -specific substrate peptide. This system can distinguish between normal and tumor cells but is not tissue-specific.¹⁸

On the other hand, Kuroda's group reported the use of bionanocapsules (BNCs) as new drug and gene delivery carriers.^{19,20} BNCs are hollow nanoparticles consisting of hepatitis B virus surface antigen molecules and a lipid bilayer. BNCs can be produced efficiently in recombinant yeast and are therefore free of other components of hepatitis B virus. The pre-S1 peptide displayed on BNCs specifically recognizes human hepatocytes.¹⁹ Several studies have reported that BNCs showed high transfection efficiency and specificity to hepatocytes or hepatoma. The in vivo pinpoint delivery of genes and drugs to human hepatoma cells using BNCs has been demonstrated in mouse xenograft experiments.^{19–21} Despite these advantages, however, BNCs are unable to distinguish between normal human hepatocytes and hepatoma cells.

In the present study we developed a novel hepatoma-targeted gene delivery system by combining our tumor cell-specific gene regulation system with human liver cell-specific BNCs. The complex showed increased transfection efficiency and selectivity for hepatoma cells, but no gene expression in normal human hepatocytes or human epidermoid tumor cells (A431).

Methods

Synthesis of polymers

For the synthesis of polymers, *N*-methacryloyl peptide (3.75 mg, 2.75 μ mol), in which the methacryloyl group is attached at the N terminus of the peptide, *N*-isopropylacrylamide (20.4 mg, 180 μ mol), and *N*-methacryloyl-polyethylene glycol (NPEG; 4.39 mg, molecular weight 12,000) were dissolved in

degassed water and allowed to stand at room temperature for 1 hour after the addition of ammonium persulfate (3.1 mg, 2.9 mmol) and *N,N,N',N'*-tetramethylethylenediamine (4 μ L, 5.8 mmol) as the redox initiator couple. The product was then purified by overnight dialysis against water using a semipermeable membrane bag (with a molecular-weight cutoff of 100,000), followed by lyophilization, to produce a white powder. The positive polymer NPEG(S) contained serine at the phosphorylation site of the peptide, but this was substituted with alanine in the negative polymer, NPEG(A); the amino acid sequence of peptides is presented in Supplementary Figure 1 (available in the online version of this article).

Monitoring of phosphorylation of polymer-DNA complex by PKC α

Determination of phosphate incorporation into NPEG(S), NPEG(A), or peptides was carried out using a coupled-enzyme assay.²² The oxidation of NADH (the reduced form of nicotinamide dinucleotide, or NAD⁺), which can be monitored spectrophotometrically as an absorbance decrease at 340 nm, was coupled to the production of adenosine diphosphate using lactate dehydrogenase and pyruvate kinase. After incubation of the polymers and peptides (final peptide concentration was 32 μ M) in 10 mM HEPES buffer (pH 7.2) containing 0.2 mM adenosine triphosphate (ATP), 10 mM MgCl₂, 1 mM phosphoenolpyruvate, 0.3 mM NADH, 10 U/ μ L lactate dehydrogenase, and 4 U/ μ L pyruvate kinase at 25°C, all reactions were initiated by the addition of activated PKC α .

Monitoring of disintegration of NPEG-DNA complex in response to PKC α

The disintegration of complexes in response to phosphorylation by PKC α was monitored by measuring the laser light scattering intensity of the complex dispersions using a Zetasizer (Malvern Instruments, Worcestershire, UK). The complex dispersions were diluted to obtain a measurement solution (15 μ L) containing 25.6 nM peptide, 1 mM MgCl₂, 0.5 mM CaCl₂, 100 μ M ATP, 2.0 mg/mL diacylglycerol, 2.5 μ g/mL phosphatidylserine, 1 ng/mL PKC α , 10 mM HEPES (pH 7.3). The reaction was initiated by adding ATP and was performed at 25°C.

Transfection of NPEG-DNA-BNC complex into cells

The NPEG-DNA complex with various cation/anion (C/A) charge ratios (0.5, 1.0, and 2.0) was prepared by mixing NPEG with 0.5 μ g of DNA for 10 minutes at room temperature and then for 5 minutes at 37°C. Next, 3 μ L of liposome solution was prepared according to the recommended procedure (COAT-SOME EL-01-D; NOF Corporation, Tokyo, Japan), mixed with the polymer-DNA solution, and incubated at room temperature for 15 minutes. The NPEG-DNA-liposome solution was then mixed with 2.5 μ g of BNCs for 15 minutes, and the resulting solution (NPEG-DNA-BNC complex) was added to cells. HuH-7 cells and normal human hepatocytes were maintained in Dulbecco's modified eagle's medium (Sigma, St. Louis, Missouri) supplemented with 10% (vol/vol) fetal bovine serum, penicillin (100 U/mL), streptomycin (100 μ g/mL), and

- amphotericin B (0.25 $\mu\text{g}/\text{mL}$) (all from Invitrogen, New York). The cells were kept in a humidified atmosphere containing 5% CO_2 and 95% air at 37°C. The medium was aspirated and changed 24 hours after addition of the complex. Fluorescence micrographs of the cells were obtained by microscopy (BZ-9000, Keyence Co., Osaka, Japan) 48 hours after transfection.
- Quantification of DNA by real-time polymerase chain reaction**
- NPEG-DNA (pCMV-luc, 1.0 μg)-BNC complexes were prepared as described above, and the complex solution was poured onto the cells. At 24 hours after addition of the complex, medium was removed and the cells were washed three times with 300 μL phosphate-buffered saline. Extraction of DNA was performed according to the protocols for the High Pure PCR Template Preparation Kit (Roche Diagnostics GmbH, Mannheim, Germany). The levels of pCMV-luc in HuH-7 cells were estimated by quantitative real-time polymerase chain reaction (PCR) (LightCycler 1.5; Roche Diagnostics, Switzerland), in which a part of the luciferase region of pCMV-luc in extracted DNA samples was amplified by PCR. Sequences of PCR primers were as follows: forward, 5'-aagatggaaccgctgaga-3' and reverse, 3'-ctcttgccaaccgacg-5'. Each PCR reaction mixture (20 μL) consisted of 2 μL DNA template (1 ng/ μL), 0.8 μL primers (10 μM stock solutions), and 10 μL SYBR Premix Ex Taq (TaKaRa Bio, Tokyo, Japan). The levels of pCMV-luc were standardized against total DNA amounts extracted from HuH-7 cells.
- Cell viability assay**
- Cell viability was determined using WST-1 reagent {4-[3-(2-methoxy-4-nitrophenyl)-2-(4-nitrophenyl)-2H-5-tetrazolio]-1,3-benzene disulfonate sodium salt} (Dojindo Laboratories, Kumamoto, Japan). HuH-7 cells were incubated in the presence or absence of the NPEG-DNA-BNC complex (C/A = 0.5, 1.0, and 2.0) or Lipofectamine 2000 (10 $\mu\text{g}/\text{mL}$)-DNA complex for 24 hours in a 48-well plate. The conditioned medium in each well was replaced with 200 μL of fresh medium containing WST-1, and cells were incubated for 3 hours. The absorbance was measured at 450 nm. The percentage cell viability was calculated by normalizing the absorbance of treated cells to that of untreated cells. The results were analyzed statistically using two-sided Student's *t*-tests.
- Animal experiments**
- Animal studies were performed in accordance with the Guidelines for Animal Experiments of Kyushu University. Male 5-week-old BALB/c nu/nu mice were used. Animals were inoculated subcutaneously with 1×10^7 tumor cells in 100 μL of Matrigel (BD Biosciences, Bedford, Massachusetts). Tumors were allowed to grow to a mean diameter of approximately 8 mm. NPEG-DNA-BNC complex containing 10 μg of DNA (C/A = 2.0) was prepared according to the method described above. A 140- μL aliquot of NPEG-DNA-BNC solution was injected directly into tumors or normal skin tissue. At 24 hours mice were anesthetized and injected intraperitoneally with 0.3 mL of 15 mg/mL D-luciferin (potassium salt; Promega, Wisconsin) in Ringer's solution. The images were obtained using a cooled C4742-98-26G02 charge-coupled device camera (Hamamatsu Photonics Systems, Hamamatsu, Japan) and analyzed for contrast and brightness using Adobe Photoshop 6.0 software. After a photographic image was taken, luminescent images were obtained from the anesthetized mice over the course of 10 minutes.
- Results**
- Synthesis of polymers, NPEG(S) and NPEG(A)**
- We earlier had succeeded in inducing tumor-specific gene expression using a polymer composed of polyacrylamide as the main chain and PKC α -specific substrate peptide as the side chain.¹⁸ In the present study the stability and size reduction of the complex was examined after the introduction of PEG units into the polymer as second side chains and the use of hydrophobic *N*-isopropylacrylamide as the main chain.^{23,24} Two conjugates, NPEG(S) and its negative control NPEG(A), were designed using a similar procedure (Supplementary Figure 1, available in the online version of this article). NPEG(A) is not phosphorylated by PKC α , because the serine residue at the phosphorylation site is substituted with alanine. NPEG(S) and NPEG(A) contained the peptide side chain at a concentration of 0.9 and 1.2 mol%, respectively, and the PEG side chain at a concentration of 0.2 mol%, as estimated by the results of proton nuclear magnetic resonance and elemental analysis. The mean diameters of NPEG(S)-DNA and NPEG(A)-DNA were <100 nm at all C/A ratios (Supplementary Table 1, available in the online version of this article).
- Disintegration of NPEG-DNA complex by the addition of PKC α**
- We investigated if NPEG(S) could act as a substrate of PKC α using a coupled-enzyme assay.²² In this assay the production of adenosine diphosphate, which is derived from ATP as a byproduct of the peptide phosphorylation, brings about the oxidation of NADH using lactate dehydrogenase and pyruvate kinase. Phosphorylation can thus be monitored by the reduction in absorbance at 340 nm. A time-dependent reduction in the absorbance at 340 nm was identified after the addition of PKC α (Figure 1, A). A reduction in absorbance at 340 nm was observed in both peptide(S) and NPEG(S)-DNA, but the absorbance remained constant in the case of peptide(A) and NPEG(A)-DNA. These results suggest that the peptide grafted in the NPEG polymer is phosphorylated by PKC α after being incorporated into the polymer backbone and combined with DNA.
- We monitored the disintegration of the NPEG(S)-DNA complex using the laser light scattering intensity. The time-dependent change in the intensity is presented in Figure 1, B. After the addition of PKC α , the intensity of NPEG(S)-DNA gradually decreased, whereas no change was detected in NPEG(A)-DNA. These results indicate that the NPEG(S)-DNA complex can be disintegrated by phosphorylation of the peptide.
- Cytotoxicity of NPEG-DNA-BNC**
- Recently, Kuroda's group succeeded in combining large materials (100-nm fluorescence-labeled polystyrene beads and >30-kilobase pair plasmids) with BNCs using a liposome

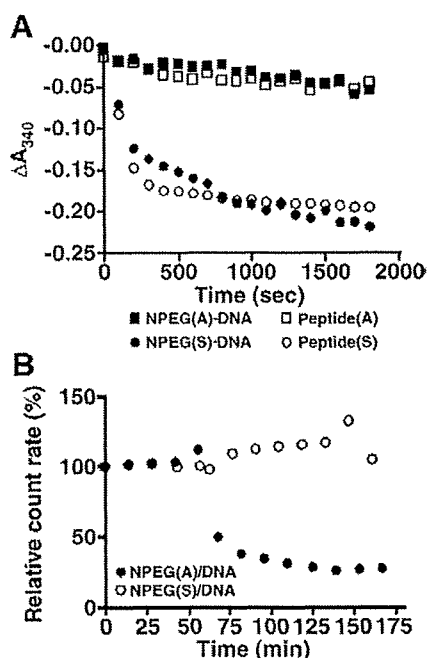


Figure 1. (A) Monitoring of phosphorylation of grafted peptide in the form of a NPEG-DNA complex or substrate peptide, using a coupled enzyme assay. The enzymatic reaction was started at 0 minutes by adding adenosine triphosphate. The charge ratio of the complex was 2.0. (B) Change of relative scattering intensity of NPEG-DNA complex dispersions after initiation of enzymatic reaction with protein kinase $C\alpha$ (PKC α).

Q12

263 composed of dioleoylphosphatidylethanolamine/cholesterol-
 264 DC-6-14.²⁰ In the present study we used the same liposome to
 265 form the NPEG-DNA complex with BNCs. BNCs are
 266 nanoparticles composed of human hepatocyte L protein
 267 embedded in a yeast endoplasmic reticulum membrane-derived
 268 phospholipid vesicle, and it is therefore able to combine
 269 effectively with the NPEG-DNA complex coated by a
 270 phospholipid liposome vesicle.²⁰

271 The cytotoxicity of NPEG-DNA-BNC was determined using
 Q11272 the WST-1 assay. The NPEG-DNA-BNC complexes showed no
 273 toxicity to cells at C/A ratios of 0.5, 1.0, and 2.0, whereas the
 Q12274 commercial transfection reagent (Lipofectamine 2000) showed
 275 significant cytotoxicity (Figure 2, A).

276 Quantification of DNA by real-time PCR

277 To investigate the transfection ability of the NPEG-DNA-
 278 BNC complex into hepatoma cells, the amounts of DNA after
 279 transfection were quantified. Cells were lysed and the amount of
 280 DNA was quantified by real-time PCR. The level of DNA
 281 transferred by NPEG(S) and BNCs was significantly higher than
 282 that by NPEG(S) alone ($P < .001$) (Figure 2, B). However, the
 283 level of DNA transferred by NPEG(S)-DNA-BNC was similar to
 284 that by NPEG(A)-DNA-BNC. These results show that the
 285 delivery of NPEG-DNA into cells was promoted by BNCs.
 286 No difference in the delivery into cells between NPEG(A)
 287 and NPEG(S) means that NPEG(A) can be used as a
 288 negative control.

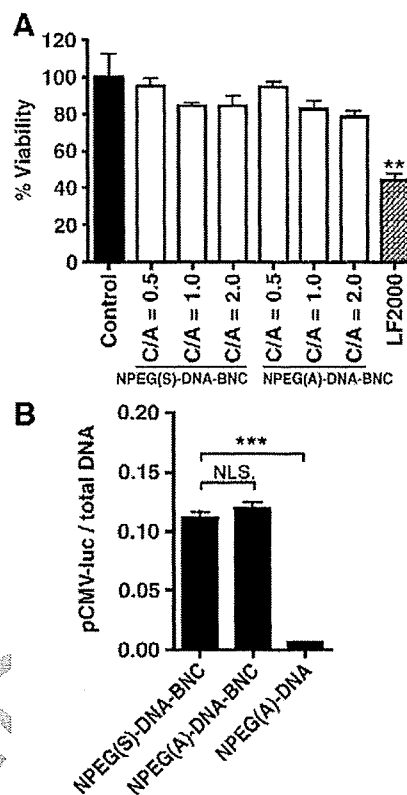


Figure 2. (A) Cytotoxicity of NPEG-DNA-BNC (charge ratio, C/A = 0.5, 1.0, and 2.0) or Lipofectamine 2000-DNA complexes toward cells. Cells were incubated for 24 hours in a 48-well plate, and cell viability was determined by WST-1 assay. The cell viability (%) was calculated by normalizing the absorbance of treated cells to that of untreated control cells. Error bars represent standard errors of the means of three experiments. Control sample (no treated cells) showed significantly higher cell viability compared with cells treated with Lipofectamine 2000 (** $P < .05$). (B) Quantification of DNA by real-time polymerase chain reaction. Cells were incubated with NPEG-DNA complexes with or without bionanocapsules (BNC) for 24 hours. Error bars represent standard errors of the means of three experiments. *** $P < .001$.

Delivery of NPEG-green fluorescent protein-encoding DNA-BNC into HuH-7 cells or normal human hepatocytes 289 290

We determined if phosphorylation by PKC α was able to 291 induce gene expression from the NPEG(S)-DNA-BNC complex 292 after transfection. HuH-7 cells were treated with NPEG(S)-GFP 293 gene-BNC, and GFP expression was examined. GFP expression 294 was observed at all C/A ratios (0.5-2.0) of NPEG(S)-DNA-BNC, 295 whereas no GFP expression was found at a C/A ratio of 2.0 in the 296 case of NPEG(A)-DNA-BNC (Figure 3). 297

Our developed gene delivery system needed to show 298 hepatoma-specific gene delivery, and no gene expression in 299 normal hepatocytes. Thus, we transfected the NPEG-DNA- 300 BNC complex into normal human hepatocytes. GFP expression 301 was observed in the DNA-BNC-transfected cells (Figure 3), 302 whereas no expression occurred after transfection of DNA 303 alone (data not shown), indicating that the BNCs had normal 304 gene transfection ability into human hepatocytes. However, 305

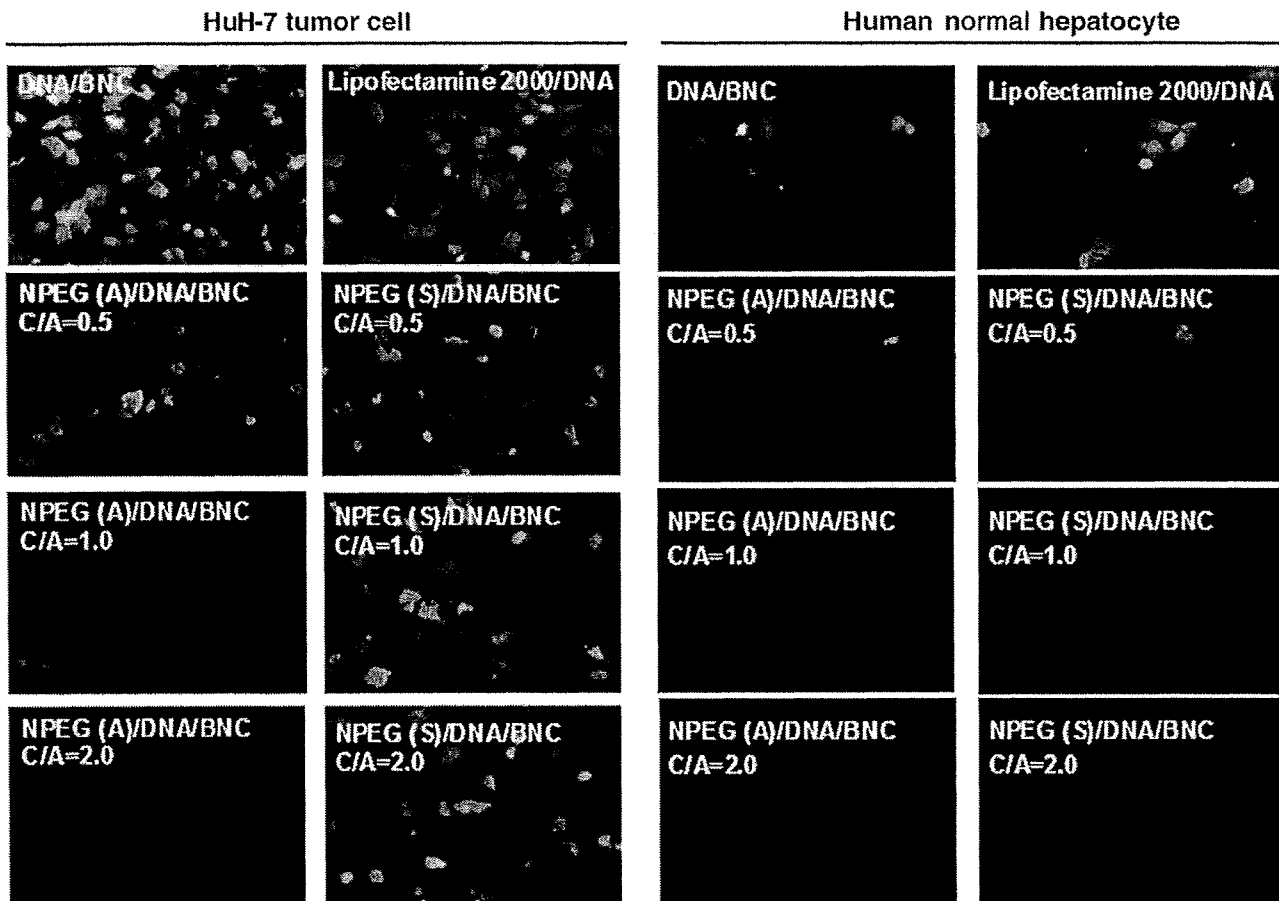


Figure 3. Green fluorescent protein (GFP) expression after transfection of NPEG-GFP-encoding DNA-BNC complex into normal human hepatocytes or HuH-7 tumor cells. C/A, charge ratio.

306 GFP expression was depressed completely when the NPEG(S)-
 307 DNA-BNC complex at a C/A ratio of 2.0 was transfected into
 308 normal human hepatocytes.

309 At C/A ratios of 0.5 and 1.0, however, gene expression was
 310 identified in NPEG(A)-DNA-BNC complex-transfected cells,
 311 which may be related to the instability of the complex.

312 *Delivery of NPEG-luciferase-encoding DNA-BNC complex* 313 *into xenografted mice*

314 On the basis of the results of the in vitro experiments, we
 315 applied our system in mice xenografted with tumors at a C/A
 316 ratio of 2.0. NPEG-luciferase gene-BNC complexes were
 317 injected directly into HuH-7 tumors or normal skin tissue of
 318 mice. Tumor-specific luciferase expression was observed with
 319 NPEG(S)-DNA-BNC. On the other hand, no expression was
 320 found in either tumor or normal tissue after injection of the
 321 negative control (NPEG(A)-DNA-BNC) (Figure 4).

322 The hepatoma specificity of the NPEG-DNA-BNC system
 323 was tested by applying it to human epidermoid tumor tissues
 324 (A431) containing activated PKC α . No gene expression was
 325 detected from A431 tumor tissues, indicating that the NPEG-
 326 DNA-BNC complex is a useful system for hepatoma-selective
 327 gene expression.

Discussion

Hepatoma-targeted therapy is an important means of
 increasing treatment efficiency and avoiding undesirable side
 effects. Intracellular signals have recently been investigated as
 therapeutic targets for hepatomas. This therapeutic approach
 involves the use of inhibitors to target specific protein kinases.
 Hepatoma cells make use of two main signal transduction
 pathways for tumor cell differentiation, proliferation, and
 survival; the RAS/RAF/MEK/ERK and the PI3K/Akt/mTOR
 pathways.^{4,6-8,25} Their various pharmacological inhibitors, such
 as sorafenib and sunitinib, have been tested extensively in
 preclinical and early-stage clinical trials for the treatment of
 hepatoma. These inhibitors have been shown to inhibit the
 promotion, as well as the proliferation, of hepatomas, but have
 poor specificity for hepatoma cells.^{4,6-8,26} Moreover, inhibitors
 of PKC isozymes (e.g., staurosporin, tamoxifen, and UCN-01),
 including PKC α , that are activated by the RAS/RAF/MEK/ERK
 and the PI3K/Akt pathways, show low specificity for hepatoma
 cells, and because these signals are involved in normal cells, their
 suppression by inhibitors leads to the development of undesir-
 able side effects.¹³⁻¹⁶ These results indicate the limitations
 associated with hepatoma cell-specific treatment using inhibi-
 tors of intracellular signals.^{4,6-8,13-16,26}

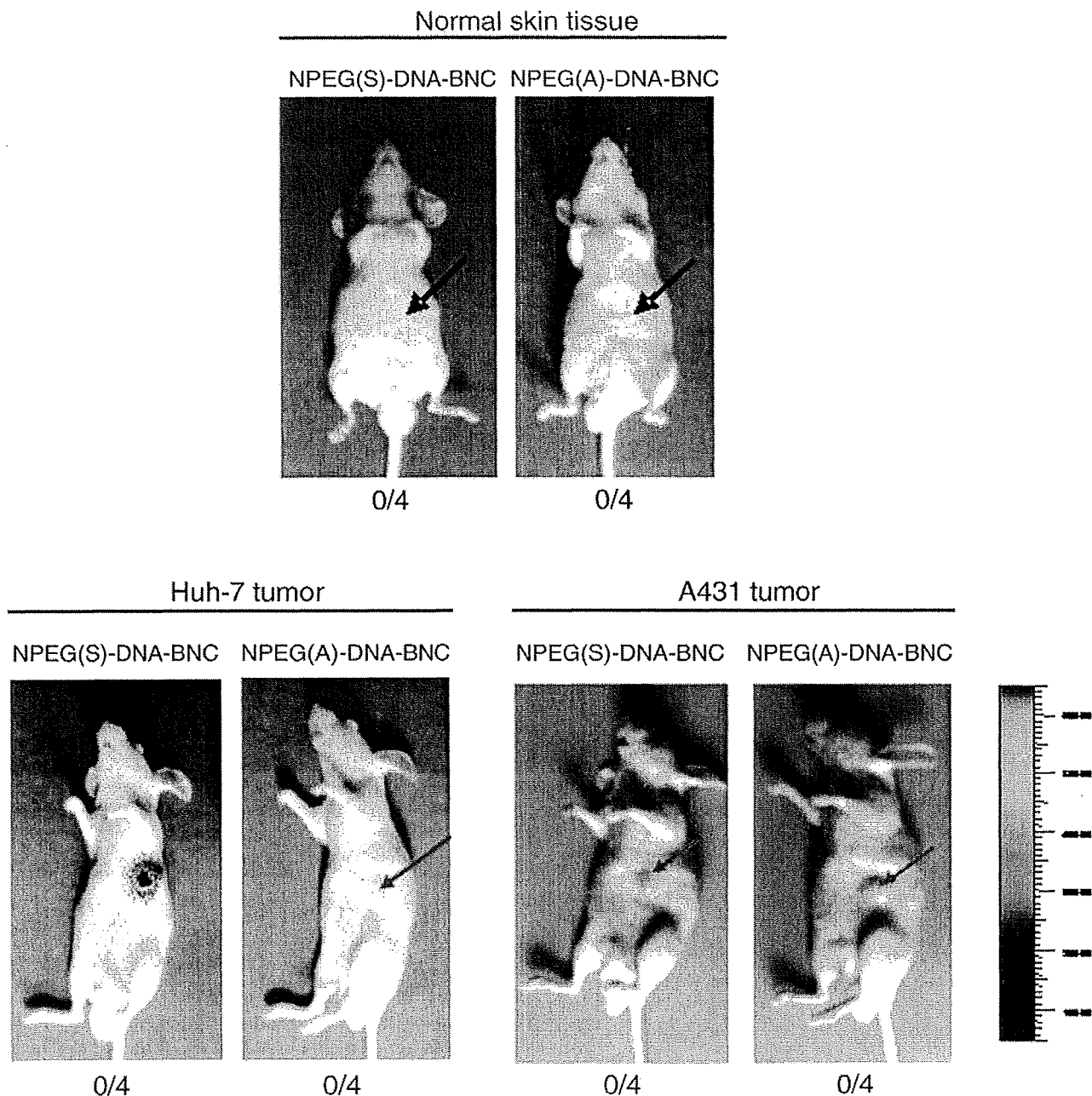


Figure 4. Luciferase activity in normal subcutaneous, xenografted HuH-7 tumors or A431 tumors 24 hours after direct injection of NPEG-DNA-BNC complexes ($C/A = 2.0$). Numbers of luciferase-expressing mice per total number of mice are described below the pictures. Arrows indicate the injection site of NPEG-DNA-BNC complexes.

351 In this study we developed a novel system for hepatoma-
 352 specific therapy using the combination of a tumor cell-specific
 353 gene regulation system responding to $PKC\alpha$, and human
 354 hepatocyte-specific BNCs. In this system, hydrophilic polymers
 355 grafted with a cationic $PKC\alpha$ -specific substrate peptide, form
 356 complexes with DNA. DNA transcription is repressed when it
 357 forms a complex with the polymer, as a result of steric hindrance.
 358 The grafted cationic peptides act as substrates for the target $PKC\alpha$,
 359 which is activated specifically in hepatoma cells. Phosphorylation
 360 by $PKC\alpha$ reduces the peptide cationic charge, resulting in release
 361 of DNA from the complex. Thus, the process of gene expression

362 involves (1) the strong binding of complexes to the surface of
 363 hepatoma cells by BNCs, (2) the transfection of complexes into
 364 the cytosol by endocytosis, and then (3) DNA release from the
 365 NPEG-DNA complex by phosphorylation of the substrate peptide
 366 by $PKC\alpha$. The NPEG-DNA-BNC complex showed no cytotoxicity
 367 to cells at all C/A ratios (0.5, 1.0, and 2.0) (Figure 2, A). Our
 368 system demonstrated hepatoma-specific gene expression both in
 369 vitro and in vivo. Interestingly, GFP expression was identified in
 370 the NPEG(S)-DNA-BNC complex-transfected hepatoma cells
 371 ($C/A = 2.0$), but no expression was detected in complex-
 372 transfected normal human hepatocytes (Figure 3). These results

373 demonstrate that this gene delivery system can distinguish
 374 between hepatoma cells and normal hepatocytes. Moreover,
 375 using mice xenografted with human tumors, we identified gene
 376 expression from hepatoma HuH-7 tumors but not from A431
 377 tumors (Figure 4) or human lung adenocarcinomas (A549) (data
 378 not shown), indicating hepatoma-selective expression. Over-
 379 expression of PKC α has already been detected in these three
 380 types of tumor cells.¹⁸ Based on these results, our novel gene
 381 regulation system has great potential for applications in hepatoma-
 382 specific gene therapy and molecular imaging.


383 Appendix A. Supplementary Material

384 Supplementary data associated with this article can be found,
 385 in the online version, at doi:10.1016/j.nano.2010.01.007.

386 References

- 387 1. Berrino F, De Angelis R, Sant M, Rosso S, Lasota M, Coebergh JW,
 388 et al. Survival for eight major cancers and all cancers combined for
 389 European adults diagnosed in 1995-99: results of the EURO-CARE-4
 390 study. *Lancet Oncol* 2007;8:773-83.
- 391 2. Jemal A, Siegel R, Ward E, Murray T, Xu J, Thun MJ. Cancer statistics,
 392 2007. *CA Cancer J Clin* 2007;57:43-66.
- 393 3. Yu AS, Keeffe EB. Management of hepatocellular carcinoma. *Rev*
 394 *Gastroenterol Disord* 2003;3:8-24.
- 395 4. Llovet JM, Bruix J. Molecular targeted therapies in hepatocellular
 396 carcinoma. *Hepatology* 2008;48:1312-27.
- 397 5. Herr I, Schemmer P, Büchler MW. On the TRAIL to therapeutic
 398 intervention in liver disease. *Hepatology* 2008;46:266-74.
- 399 6. Hui KM. Current approaches in the transcriptional-guided gene therapy
 400 of human hepatocellular carcinoma. *Curr Opin Mol Ther* 2007;9:378-84.
- 401 7. Avila MA, Berasain C, Sangro B, Prieto J. New therapies for
 402 hepatocellular carcinoma. *Oncogene* 2006;25:3866-84.
- 403 8. Calvisi DF, Pascale RM, Feo F. Dissection of signal transduction
 404 pathways as a tool for the development of targeted therapies of
 405 hepatocellular carcinoma. *Rev Recent Clin Trials* 2007;2:217-36.
- 406 9. Riki T, Kang JH, Kim JH, Tomiyama T, Mori T, Niidome T, et al. Protein
 407 kinase C α -specific peptide substrate graft-type copolymer for cancer cell-
 408 specific gene regulation systems. *J Control Release* 2009;139:133-9.
- 409 10. Kawamura K, Oishi J, Kang JH, Kodama K, Sonoda T, Murata M, et al.
 410 Intracellular signal-responsive gene carrier for cell-specific gene
 411 expression. *Biomacromolecules* 2005;6:908-13.
- 412 11. Oishi J, Kawamura K, Kang JH, Kodama K, Sonoda T, Murata M, et al.
 413 An intracellular kinase signal-responsive gene-carrier for cell specific
 414 gene therapy. *J Control Release* 2006;110:431-6.
- 415 12. Manning G, Whyte DB, Martinez R, Hunter T, Sudarsanam S. The
 416 protein kinase complement of the human genome. *Science* 2002;298:
 417 1912-34.
- 418 13. Cohen P. Protein kinases—the major drug targets of the twenty-first
 419 century? *Nat Rev Drug Discov* 2002;1:309-15.
- 420 14. Hofmann J. Protein kinase C isozymes as potential targets for anticancer
 421 therapy. *Curr Cancer Drug Targets* 2004;4:125-46.
- 422 15. Goekjian PG, Jirousek MR. Protein kinase C inhibitors as novel
 423 anticancer drugs. *Expert Opin Investig Drugs* 2001;10:2117-40.
- 424 16. O'Brian CA, Chu F, Bornmann WG, Maxwell DS. Protein kinase C α
 425 and ϵ small-molecule targeted therapeutics: a new roadmap to two holy
 426 grails in drug discovery? *Expert Rev Anticancer Ther* 2006;6:175-86.
- 427 17. Kang JH, Asai D, Yamada S, Toita R, Oishi J, Mori T, et al. A short
 428 peptide is a protein kinase C (PKC) α -specific substrate. *Proteomics*
 429 2008;8:2006-11.
- 430 18. Kang JH, Asai D, Kim JH, Mori T, Toita R, Tomiyama T, et al. Design
 431 of polymer carriers for cancer-specific gene targeting: utilization of
 432 abnormal protein kinase C α activation in cancer cells. *J Am Chem Soc*
 433 2008;130:14906-7.
- 434 19. Yamada T, Iwasaki Y, Tada H, Iwabuki H, Chuah MKL, Vanden-
 435 Driessche T, et al. Nanoparticles for the delivery of genes and drugs to
 436 human hepatocytes. *Nat Biotechnol* 2003;21:885-90.
- 437 20. Jung J, Tatematsu K, Matsuzaki T, Okajima T, Ueda M, Kondo A, et al.
 438 Bio-nanocapsule conjugated with liposomes for in vivo pinpoint delivery
 439 of various materials. *J Control Release* 2008;125:255-64.
- 440 21. Kasuya T, Jung J, Kadoya H, Matsuzaki T, Tatematsu K, Okajima T,
 441 et al. In vivo delivery of bionanocapsules displaying *Phaseolus*
 442 *vulgaris* agglutinin-L4 isolectin to malignant tumors overexpressing
 443 *N*-acetylglucosaminyltransferase V. *Hum Gene Ther* 2008;19:887-95.
- 444 22. Cook PF, Neville ME, Vrana KE, Hartl FT, Roskoski R. Adenosine
 445 cyclic 3',5'-monophosphate dependent protein kinase: kinetic mecha-
 446 nism for the bovine skeletal muscle catalytic subunit. *Biochemistry*
 447 1982;21:5794-9.
- 448 23. Kumar TR, Soppimath K, Nachaegari SK. Novel delivery technologies
 449 for protein and peptide therapeutics. *Curr Pharm Biotechnol* 2006;7:
 450 261-76.
- 451 24. Jeong B, Kim SW, Bae YH. Thermosensitive sol-gel reversible
 452 hydrogels. *Adv Drug Deliv Rev* 2002;54:37-51.
- 453 25. Boyault S, Rickman D, de Reynies A, Balabaud C, Rebouissou S,
 454 Jeannot E, et al. Transcriptome classification of HCC is related to gene
 455 alterations and new therapeutic targets. *Hepatology* 2007;45:42-52.
- 456 26. Tommasi S, Pinto R, Pilato B, Paradiso A. Molecular pathways and
 457 related target therapies in liver carcinoma. *Curr Pharm Des* 2007;13:
 458 3279-87.
- 459

AUTHOR QUERY FORM

 ELSEVIER	Journal: NANO	Please e-mail or fax your responses and any corrections to: Angela Stafford E-mail: stafforda@cadmus.com Tel: 717-738-9335 Fax: 717-738-9479 or 717-738-9478
	Article Number: 335	

Dear Author,

Any queries or remarks that have arisen during the processing of your manuscript are listed below and highlighted by flags in the proof. Please check your proof carefully and mark all corrections at the appropriate place in the proof (e.g., by using on-screen annotation in the PDF file) or compile them in a separate list.

For correction or revision of any artwork, please consult <http://www.elsevier.com/artworkinstructions>.

Articles in Special Issues: Please ensure that the words 'this issue' are added (in the list and text) to any references to other articles in this Special Issue.

Uncited references: References that occur in the reference list but not in the text – please position each reference in the text or delete it from the list.	
Missing references: References listed below were noted in the text but are missing from the reference list – please make the list complete or remove the references from the text.	
Location in article	Query / remark Please insert your reply or correction at the corresponding line in the proof
Q1	Please check refs 19, 20. Kuroda's name not shown.
Q2	Okay to add NPEG here, because this is where you define it? See also figure legends.
Q3	Please supply a temperature range for "room temperature."
Q4	Please provide city in New York state where Invitrogen is located.
Q5	Please provide city in Switzerland where Roche Diagnostics (supplier of LightCycler 1.5) is located.
Q6	Please supply the manufacturer and location (city and state if in the US, or city and country, if outside of the US) for Lipofectamine 2000.
Q7	Pls define NPEG, Peptide(S), and Peptide(A).
Q8	Please clarify what is meant by the (A) and (S) in peptide(A) and peptide(S).
Q9	Please clarify what is meant by the (A) and (S) in peptide(A) and peptide(S).
Q10	Please check refs 19, 20. Kuroda's name not shown.
Q11	Okay to change WST to WST-1 as before?
Q12	Please supply the manufacturer for Lipofectamine 2000.

Electronic file usage

Sometimes we are unable to process the electronic file of your article and/or artwork. If this is the case, we have proceeded by:

6. ぶどう膜炎治療におけるドラッグデリバリーシステムの可能性

— The potentiality of DDS in uveitis treatment —

真 下 永* 黒田 俊一**

はじめに

ぶどう膜炎では少なからぬ症例で慢性に経過し、長期にわたりステロイドを含む免疫抑制剤の全身投与が行われる場合がある。これらの症例では免疫抑制剤による全身への副作用がしばしば問題となる。

薬物の効果は体内に投与された薬物が、目的とする標的部位に到達することによって発現する。免疫抑制剤の全身投与では、体内に投与された薬物は目的とする標的部位にまで効率的に到達することができないばかりか、代謝・排泄を受けたり、ある部位にトラップされたりするので、有効濃度を維持することが困難である。

このため、薬理活性を示すに必要な濃度を全身において維持するために、投与する薬物量は多くなり、副作用が生じてしまう。標的性のある製剤を調製し、標的部位において薬剤が有効濃度に達するように調整すると、このような欠点を克服することができる。

このように「必要なときに、必要な量の薬剤

を、必要とする部位に到達させる」仕組みがドラッグデリバリーシステム (drug delivery system: DDS) である。

実はぶどう膜炎治療においては既にさまざまな局所投与による DDS が存在する。ステロイド剤点眼は非侵襲的に前眼部に薬剤を到達させるための理想的な DDS である。また後眼部に対しても、トリアムシノロンアセトニドのテノン嚢下注射および硝子体注射、ステロイド徐放製剤の眼内インプラント等の DDS があり、ぶどう膜炎治療において有用である。

しかし、これら局所投与による DDS では眼局所の副作用 (易感染性、ステロイド緑内障、白内障) 等の頻度が高く、後眼部に対する治療は患者における侵襲も大きいと考えられる。その適応に対しては慎重に考えざるを得ないのが現状である。また、局所投与故に、全身免疫疾患 (サルコイドーシス、ベーチェット病、原田病等) においては眼以外の炎症部位への治療効果は期待できず、眼局所の消炎も不十分となる症例も存在する。

また、慢性ぶどう膜炎においては長期にわたる治療が必要となり、遺伝子治療が可能となれば有用と考えられる。遺伝子治療においても、いかに必要な時に必要な量の遺伝子を必要とする部位に到達させるか (gene delivery system:

* Hisashi MASHIMO 大阪大学大学院医学系研究科眼科学分野

** Shunichi KURODA 名古屋大学大学院生命農学研究科産業生命工学研究分野

Key words: バイオナノカプセル, ドラッグデリバリーシステム, ぶどう膜炎, bio-nanocapsule, DDS, uveitis

GDS) が重要であるが、ぶどう膜炎治療においてはほぼ未開拓な領域である。

これらのことを踏まえると投与ルートが確保しやすい静脈注射を行うことで炎症病巣における薬物、遺伝子の集積を高め、長期間その効果を維持できる DDS/GDS が可能となれば理想的な炎症抑制療法となることが考えられる。

本項では、そうした DDS を可能とする「生体内における細胞および組織への薬剤標的化技術 (*in vivo targeting*)」を概説するとともに、その技術の中で、筆者らが開発したウイルス法とリポソーム法のハイブリッド型である「バイオナノカプセル法 (bio-nanocapsule : BNC)」を紹介する。BNC 法は、低分子化合物、遺伝子、蛋白質などのさまざまな薬物を包含することができる全く新しいキャリアー(運搬体)であり、今後の医薬品を革新的に変えてゆくと期待されている *in vivo pinpoint drug/gene delivery system* (薬剤および遺伝子の生体内ピンポイント投与システム) のプラットフォーム技術である。次に実験的自己免疫性ぶどう膜炎モデルに対してこの技術を応用し、DDS 製剤としての BNC の有用性を報告する。

1. *In vivo targeting* を達成する技術

① EPR 効果

In vivo targeting の実現には、2段階の技術的問題をクリアーしないとイケない。①生体内に投与された薬剤(遺伝子を含む)を、血流により目的の臓器および組織に到達させる技術(マクロレベルの標的化技術)と、②臓器および組織内部で正常細胞と目的細胞(target cells)を見分けて、目的細胞だけに薬剤を導入、もしくは作動させる技術(ミクロレベルの標的化技術)が必要である。まず、マクロレベルの標的化技術としては、EPR 効果 (enhanced permeation and retention effect) がある。これは、癌組織に含

まれる新生血管の血管壁細胞間隙が正常組織とは異なり 100 nm より大きいことから、血流中を循環する直径約 100 nm の物質が癌組織内の血管壁外に浸潤して、次第に癌組織に蓄積する現象である。既にリポソーム、高分子ミセルからなる直径 100 nm のキャリアーが開発されており、内部に抗癌剤を包含させ、EPR 効果により癌組織特異的な抗癌剤の送達に成功している。ぶどう膜炎においても血管壁細胞間隙が拡大している炎症部位で同様の効果が期待できる。実際、生体分解性高分子(ポリ乳酸、ポリグリコール酸ポリマー)から作製したマイクロステロイドをぶどう膜炎モデル動物に投与し、リン酸ベタメタゾンを炎症部位に集積させることに成功している¹⁾。ただしこうしたキャリアーは血管壁外の組織の特定の細胞を標的化できるわけではない。特に遺伝子の導入においてはこの点が問題となると考えられる。

次にミクロレベルの標的化技術としては、薬剤(遺伝子を含む)を目的細胞のみならず正常細胞にも導入するが、正常細胞では作動させず、目的細胞のみで作動させる技術(図 1A, B) や、正常細胞と目的細胞の表層状態の差を見分けて、目的細胞のみに薬剤(遺伝子を含む)を導入する技術〔能動的標的化 (active-targeting), 図 1C〕などがある。なお、後述する BNC 技術は、EPR 効果以外にさまざまな生体認識分子をキャリアー表面に提示することで能動的標的化を実現している。

② 目的細胞特異的な遺伝子発現技術

欧米で行われている遺伝子治療の現場において使用されている治療用遺伝子のキャリアーは、広範な細胞に感染することができるアデノウイルス、レトロウイルス、HIV ウイルス、アデノ随伴ウイルスなどがある。実験的ぶどう膜炎モデルラットにインターロイキン 10 をアデノウイルスベクターを用いて導入し消炎効果を認め

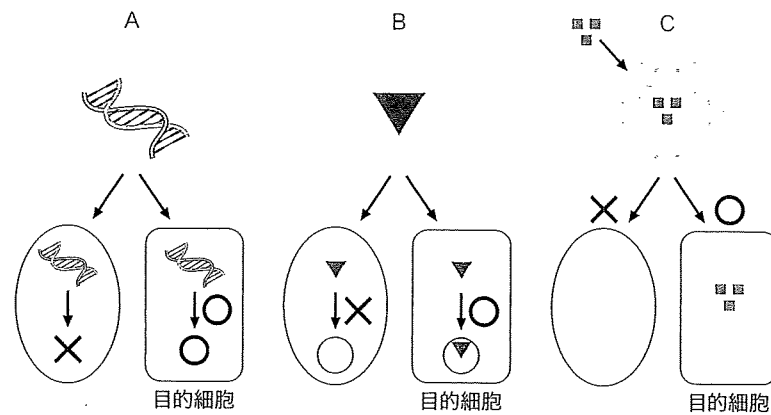


図1 ミクロレベルの標的化技術

- A: 目的細胞特異的な遺伝子発現
 B: 目的細胞特異的な薬剤活性化
 C: 目的細胞特異的な薬剤送達 (能動的標的化(active targeting))

たことが報告されている²⁾。またイギリスやアメリカではアデノ随伴ウイルスを用いた Leber 先天盲に対する遺伝子治療が開始されている³⁾。ただこれらのキャリアーは、生体内において高い感染性を有するので、患部以外の部位に対して望まれない遺伝子導入を行うことがある。つまり宿主細胞域がきわめて広範で能動的な標的化能力はほとんどない。そのために、臨床応用に際しては、たとえ目的細胞以外に治療用遺伝子が導入されても作動しないようにするフェイルセーフの機構が必要である。具体的には、治療用遺伝子の発現ベクターに含まれるプロモーター (promoter) やエンハンサー (enhancer) を目的細胞特異的に作動するように工夫されている (図 1A)。具体的には、albumin promoter および α -1-antitrypsin promoter などが肝臓特異的なプロモーターとして、また、 α -fetoprotein enhancer が肝臓特異的なプロモーターとして *in vivo* 系でも使用可能なことが示されている⁴⁾が、概して発現制御の緩いものが多いことから、現実的にはウイルスベクターと本技術のみで *in vivo* pinpoint gene therapy (生体内の任意の組織および細胞を対象とするピンポイント遺伝子治療) を達成するのは困難と考えられている。

その他に目的細胞特異的な遺伝子発現技術として細胞内シグナル応答性ポリマーがある。目的細胞内のみで遺伝子発現を行うため、すべての細胞に DNA・ポリマー複合体を導入したのち、目的細胞特異的な細胞内シグナルに応答して複合体の安定性を変化させて、DNA を作動可能な状態で目的細胞内に放出する方法が報告された⁵⁾。

④ キャリアーを用いた能動的標的化技術

1) ウイルスベクター法

ウイルスは宿主細胞に感染して自分自身の遺伝子を導入して増幅することから、ウイルスゲノム内に治療用遺伝子を組み込むことで遺伝子キャリアー (別名ウイルスベクター) として、患部に遺伝子を送達させることが広く行われている。細胞内への遺伝子導入効率は、ウイルスの感染機構を利用するため他の遺伝子キャリアーに比べて通常高いのでウイルスベクターの能動的標的化技術の開発が進んでいる。具体的には、センダイウイルスの表面に磁性ナノ粒子を付加して、磁力の作用により組織特異的な導入効率を向上させた報告がある⁶⁾。また、癌細胞を認識するペプチドをバキュロウイルスの表面に提示して、*in vitro* ながら遺伝子を癌細胞特異的に

送達した報告もある⁷⁾。しかし、これらの改変型ウイルスベクターを臨床応用するには、相当高度な生体内標的化技術を実現しないと、依然としてウイルスベクター本来の課題が残る。まず、ウイルスベクターは概して大量生産が困難であり、生産者への感染事故を防ぐ方策も必要なので、医薬品として生産するコストが非常に高くなる。また、ヒトはさまざまなウイルスに感作されているので、投与時にアナフィラキシーショックを起こす可能性が高い。さらに、ウイルスゲノム由来の遺伝子を同時に投与するので、患者の正常な遺伝子情報をかく乱する可能性がある。実際に、ウイルスベクターを利用した臨床応用で白血病の発症例⁸⁾や死亡例⁹⁾の報告がある。

2) 非ウイルスベクター法

上述したウイルス由来の副作用を回避し、飛躍的に安全性を高めるために非ウイルスベクター法が開発された。最も代表的なものはリポソームであり、安全性の向上以外にも、大量生産が容易で、遺伝子から低分子化合物までさまざまな物質を導入可能なことが長所である。しかし、リポソームの細胞内への導入効率は endocytosis によるためウイルスと比較してきわめて低く、また広範な種類の細胞に取り込まれる。

そこで橋田らは炎症血管内皮細胞特異的に発現する E-selectin を標的として、そのリガンドであり白血球の膜表面にも存在するシアリル路易斯 X を結合した標的指向性の高いリポソームを開発し、ぶどう膜炎動物モデルにて薬剤を能動的に炎症部位に集積させることに成功した¹⁰⁾。ただし、生体内における能動的標的化を実現した非ウイルスベクター法はきわめて少ないのが現状である。

リポソーム以外にもさまざまな材料を用いたポリマーが非ウイルスベクター法として使われている。たとえば、DNA と複合体を形成する

カチオン性ポリマーであるキトサン¹¹⁾¹²⁾、ポリエチレンイミン¹³⁾、poly-L-lysine¹⁴⁾¹⁵⁾、などが DNA 導入用キャリアーとして使用されている。これらのキャリアーに細胞および組織特異性を持たせるために、さまざまな工夫がされている。たとえば、ガラクトシル化¹⁶⁾¹⁷⁾やガラクトースへの置換¹⁸⁾による肝細胞への標的化、EGFR 親和性ペプチドとの結合によるヒト癌細胞への標的化¹⁹⁾、なども報告されている。しかしながら、これらのカチオン性ポリマーは核酸には適しているが他の物質に不向きな場合も多く、時々強い細胞毒性を示すことがあり、生体内において非特異的に細胞に取り込まれる性質を有するために標的化の課題が残っている。

3) バイオナノカプセル技術

ウイルスベクターや非ウイルスベクターには、上述したとおり一長一短があり、いまだ決定的な薬剤キャリアーは開発されていない。その中で、われわれのグループが従来のキャリアーの欠点を解決した新たなキャリアー「バイオナノカプセル(BNC)」の開発に成功した。

II. バイオナノカプセル技術

① バイオナノカプセルとは

BNC とは、B 型肝炎ウイルス (hepatitis B virus : HBV) の外皮蛋白質 (HBV surface antigen : HBsAg) を出芽酵母等の真核生物細胞で発現させた際に宿主由来の小胞体脂質二重膜上に膜蛋白質として存在し、出芽形式でルーメン側に直径約 100 nm の中空粒子を形成したものである (図 2)。HBsAg 蛋白質として、S 蛋白質 (226 アミノ酸残基) の N 末端側に pre-S2 領域 (55 アミノ酸残基) と pre-S1 領域 (108 アミノ酸残基) が付加した L 蛋白質を通常用いている。そのうち、pre-S1 領域の N 末端側約 70 アミノ酸残基にはヒト肝臓特異的なレセプターが存在し、HBV の厳密なヒトおよびチンパンジー肝臓